Computational Fluid Dynamics '92, Volume 1
Ch. Hirsch et al. (Editors)

ANALYSIS OF TWO FAST-CHEMISTRY COMBUSTION MODELS AND TURBULENCE MODELING IN VARIABLE DENSITY FLOW

J. NISBET, L. DAVIDSON and E. OLSSON

Dept. of Thermo and Fluid Dynamics, Chalmers University of Technology, S-412 96 Gothenburg, Sweden

Predictions have been obtained for the flow field and combustion within a non-premixed, axisymmetrical combustor without swirl. Two fast-chemistry models have been analyzed : an eddy break-up model, the Eddy Dissipation Concept (EDC), and a flame-sheet model, the Conserved Scalar approach (CS).

Generally, independent of chemistry model, the strength of both the mean and fluctuating velocities' flow fields was underpredicted in the initial mixing region, where a recirculation zone is formed of the fuel and oxygene co-flowing streams. However, the CS model, which account for the effects of turbulence on the concentration fluctuations, was found to give predictions in closer agreement with the measured flow fields than the EDC model. The discrepancies between calculated and measured flow fields are probably mainly attributable to the steady state assumption. High-speed pictures of the reacting flow field in the experiments show significant fluctuations in the turbulent structure, and the presence of large scale motions.

The sensitivity to inlet conditions has been examined, and the calculations show that an increase of the inlet turbulent intensity yields a stronger and shorter recirculation zone. This effects was much more pronounced when the CS model was used.

The turbulence is simulated by three types of $k-\varepsilon$ models. The incompressible $k-\varepsilon$ model (model 1) is extended to account for variable-density effects (model 2). A new ε- equation, proposed in (ref. 1), to include the effects of compression on dissipation of turbulent kinetic energy, has been implemented (model 3). The new model gave significant changes of the predicted flow field in the recirculation zone.

1. INTRODUCTION

Interaction between turbulence and combustion is very important in the design process of combustion chambers. Combustion phenomena and important design parameters such as wall heat transfer to the combustor lines, pollutant formation, outlet temperature distribution and combustion efficiency are governed by this interaction.

In order to avoid the problems involved with complex chemistry, a fast-chemistry assumption is made, which implies that the turbulent time scale is much longer than the time scale for reaction. Thus, the reaction takes place in a one-step, irreversible reaction, as soon as the reactants are mixed, as follow:

$$Fuel + Oxydant \rightarrow Products \qquad (1)$$

As a consequence of the fast-chemistry assumption, almost the whole turbulence spectra remains unaffected of the chemical reaction. Analysis of two different concepts of combustion modeling are presented: the Eddy Dissipation Concept (EDC) and the Conserved Scalar (CS) approach.

In the EDC chemistry model, the fuel consumption rate is determined by how fast the reactants can be transported from large to small turbulence scales, where the chemical reaction occurs if the reactants are sufficiently heated (ref. 2). The local reaction rate is therefore proportional to the eddy break-up time and the mean concentrations of the limiting species.

In the CS chemistry model, the reaction is assumed to take place in a small, continuous flame sheet, which separates the reactants (ref. 3). The turbulence wrinkles the instantaneous flame, and fluctuations in the composition due to turbulence are handled in a statistical way, by introducing a probability density function (pdf). The shape of pdf is determined from the mean and variance of species present.

The turbulence is simulated using three types of $k-\varepsilon$ models:

- model 1: the standard $k-\varepsilon$-model for incompressibel flow.
- model 2: extended to account for variable-density effects, such as pressure-density interaction, which give rise to acceleration effects, and dilation as the velocity divergence is not equal to zero.
- model 3: a new ε-equation, derived in (ref. 1), is investigated.

The new ε-equation accounts for the effects of the additional normal strain rates, owing to dilatation, on the energy dissipation ε. It is derived from the expression for conservation of angular momentum of turbulence during normal deformations,

$$\frac{k^2}{\varepsilon} = const., \tag{2}$$

and it is assumed that that the angular momentum of the different eddies is distributed very fast by the interaction between the eddies.

2. MATHEMATICAL MODELING

2.1 Mean flow equations

The mean flow is assumed to be steady and with low Mach-number, and for simplicity density-weighted averaged forms of the equations are used. As density-weighted statistics (i.e. Favre-averaged or mass-averaged) are used, correlations involving density do not appear and the final equations will thus have the same form as the constant-density time-averaged equations (ref. 4). The equations for continuity and conservation of momentum, chemical species and energy may be written as

$$\frac{\partial}{\partial x_i}\left(\overline{\rho}\tilde{U}_i\right) = 0 \tag{3}$$

$$\frac{\partial}{\partial x_j}\left(\overline{\rho}\tilde{U}_i\tilde{U}_j\right) = -\frac{\partial \overline{p}}{\partial x_i} + \frac{\partial}{\partial x_j}\left\{(\mu+\mu_t)\frac{\partial \tilde{U}_i}{\partial x_j}\right\} \tag{4}$$

$$\frac{\partial}{\partial x_j}\left(\overline{\rho}\tilde{U}_j\tilde{Y}_\alpha\right) = \frac{\partial}{\partial x_j}\left\{\left(\overline{\rho}D_\alpha + \frac{\mu_t}{\sigma_t}\right)\frac{\partial \tilde{Y}_\alpha}{\partial x_j}\right\} + \overline{w}_\alpha \tag{5}$$

$$\frac{\partial}{\partial x_j}\left(\overline{\rho}\tilde{U}_j\tilde{h}\right) = \frac{\partial}{\partial x_j}\left\{\left(\frac{\lambda}{c_p} + \frac{\mu_t}{\sigma_t}\right)\frac{\partial \tilde{h}}{\partial x_j}\right\} + \tilde{S}_h \tag{6}$$

The horizontal bar denotes time-averaged values and the tilde bar density-averaged ones, $\tilde{U}_i$ is the velocity vector, μ_t the turbulent dynamic viscosity, σ_t the turbulent Prandtl number, $\tilde{Y}_\alpha$ is the mass fraction, D_α the diffusion coefficient and $\overline{w}_\alpha$ the reaction rate of species α, respectively. $\tilde{S}_h$ is the source term appearing in the energy equation. Furthermore, $\overline{p}$ is the pressure, $\overline{\rho}$ the mean density of the gas mixture, and h is the enthalpy defined as

$$h = c_p T + Y_F \Delta H_F. \tag{7}$$

Finally, the mixing between fuel and oxydant are described using the mixing rate, ξ, defined as the mass fraction of burnt or unburnt fuel. Consequently, ξ=1 in the fuel stream, and ξ=0 in the air stream. It is assumed, as the flow is highly turbulent, that the diffusion coefficients for the different species are equal to a single value D. Thus, the averaged transport equations for the mixing rate, $\tilde{\xi}$, and its variance, $\widetilde{\xi''^2}$, becomes

$$\frac{\partial}{\partial x_j}\left(\overline{\rho}\tilde{U}_j\tilde{\xi}\right) = \frac{\partial}{\partial x_j}\left\{\left(\overline{\rho}D + \frac{\mu_t}{\sigma_t}\right)\frac{\partial \tilde{\xi}}{\partial x_j}\right\} \tag{8}$$

$$\begin{aligned}\frac{\partial}{\partial x_j}\left(\overline{\rho}\tilde{U}_j\widetilde{\xi''^2}\right) &= \frac{\partial}{\partial x_j}\left\{\left(\overline{\rho}D + \frac{\mu_t}{\sigma_t}\right)\frac{\partial \widetilde{\xi''^2}}{\partial x_j}\right\} \\ &+ 2\frac{\mu_t}{\sigma_t}\left(\frac{\partial \tilde{\xi}}{\partial x_k}\frac{\partial \tilde{\xi}}{\partial x_k}\right) - C_g\overline{\rho}\frac{\varepsilon}{k}\widetilde{\xi''^2},\end{aligned} \tag{9}$$

where the constant C_g=2.

2.2 Combustion models

2.2.1 Flame-sheet model: In the present work a novel way, proposed in (ref. 5), of including the effects of non-adiabatic phenomena is adopted. With the assumption of fast chemistry, the chemical time scales are small as compared with the turbulent mixing scales. This implies that the instantaneous mass fractions, temperature and density are functions of the instantaneous mixing rate and enthalpy. Hence,

$$Y_\alpha = Y_\alpha(\xi,h), \quad T = T(\xi,h), \quad \rho = \rho(\xi,h). \tag{10}$$

It is assumed that there is a strong correlation between the fluctuations of ξ and h, so that the two-dimensional pdf $\tilde{P}(\xi,h)$, can be reduced to the one-dimensional $\tilde{P}(\xi)$. The correlation $h(\xi)$ is taken as a quadratic function defined of

$$\begin{aligned} h(0) &= h_{air\ inlet}, \\ h(1) &= h_{fuel\ inlet}, \\ \tilde{h} &= \int_0^1 h(\xi)\tilde{P}(\xi)d\xi. \end{aligned} \tag{11}$$

Now the averaged density, mass fractions, and temperature are obtained through:

$$\frac{1}{\overline{\rho}} = \int_0^1 \frac{1}{\rho(\xi,h(\xi))}\tilde{P}(\xi)d\xi \tag{12}$$

$$\tilde{Y}_\alpha = \int_0^1 Y_\alpha(\xi, h(\xi))\,\tilde{P}(\xi)d\xi \tag{13}$$

$$\tilde{T} = \int_0^1 T(\xi, h(\xi))\,\tilde{P}(\xi)d\xi \tag{14}$$

In the present calculations a β-function pdf is employed:

$$\tilde{P}(\xi) = \frac{\xi^{a-1}(1-\xi)^{b-1}}{\int_0^1 \xi^{a-1}(1-\xi)^{b-1}d\xi}, \tag{15}$$

where the coefficients a and b are calculated from

$$a = \tilde{\xi}\{\tilde{\xi}(1-\tilde{\xi})/\widetilde{\xi''^2} - 1\}, \quad b = a(1-\tilde{\xi})/\tilde{\xi}. \tag{16}$$

2.2.2 Eddy break-up model: In the EDC chemistry model, the purpose is to model the transport of reactants to the fine structures, i.e. to the smallest scales in the flow, where, when the temperature is sufficiently high, reaction occurs. The following expression for the rate of combustion is proposed in (ref. 2) reads:

$$(\overline{w}_F)_{EDC} = -\overline{\rho}\dot{m}\frac{\kappa}{1-\gamma^*\kappa}\tilde{Y}_L, \tag{17}$$

where $\dot{m}$ is the transfer of mass per unit mass and unit time between the smallest scales in the flow and the surroundings, and $\tilde{Y}_L$ is the lesser of $\tilde{Y}_F$ and $\tilde{Y}_O/r$ where r is the stoichiometric coefficient. Further, γ^* is the volume fraction of fine structure, and κ is the fraction of the fine structure which is sufficiently heated to react.

The fuel mass fraction $\tilde{Y}_F$ is calculated from its own transport equation (equation(5)). The oxygene and product mass fractions, $\tilde{Y}_O$ and $\tilde{Y}_P$, can now be obtained through coupling functions, as the mixture- and the fuel mass fractions are known (ref. 6). As the EDC chemistry model does not account for the effect of turbulence on the concentration fluctations, i.e. the variance of the mean properties, the variance of mixture fraction is not calculated (equation(9)).

The mean density is calculated from the equation of state:

$$\overline{\rho} = \frac{\overline{p}}{R\tilde{T}\sum_{\alpha=1}^{N}(\tilde{Y}_\alpha/M_\alpha)}, \tag{18}$$

where R is the gas constant of the mixture, and M_α is the molecular mass of species α.

2.3 Turbulence modeling

The basic transport equations for k, the turbulence kinetic energy, and ε, the dissipation rate of turbulence kinetic energy, are

$$\begin{aligned}\overline{\rho}\tilde{U}_j\frac{\partial k}{\partial x_j} &= \frac{\partial}{\partial x_j}\left\{\left(\mu+\frac{\mu_t}{\sigma_k}\right)\frac{\partial k}{\partial x_j}\right\} \\ &- \overline{\rho}\widetilde{u_i''u_j''}\frac{\partial \tilde{U}_i}{\partial x_j} - \underbrace{C_3\frac{\mu_t}{\overline{\rho}^2}\frac{\partial\overline{p}}{\partial x_i}\frac{\partial\overline{\rho}}{\partial x_i}}_{1} - \overline{\rho}\varepsilon\end{aligned} \tag{19}$$

$$\begin{aligned}\overline{\rho}\tilde{U}_j\frac{\partial \varepsilon}{\partial x_j} &= \frac{\partial}{\partial x_j}\left\{\left(\mu+\frac{\mu_t}{\sigma_\varepsilon}\right)\frac{\partial \varepsilon}{\partial x_j}\right\} \\ &- C_1\frac{\varepsilon}{k}\left\{\overline{\rho}\widetilde{u_i''u_j''}\frac{\partial \tilde{U}_i}{\partial x_j} + \underbrace{C_3\frac{\mu_t}{\overline{\rho}^2}\frac{\partial\overline{p}}{\partial x_i}\frac{\partial\overline{\rho}}{\partial x_i}}_{1}\right\} \\ &- C_2\overline{\rho}\frac{\varepsilon^2}{k} + \underbrace{C_4\overline{\rho}\varepsilon\frac{\partial \tilde{U}_k}{\partial x_k}}_{2}.\end{aligned} \tag{20}$$

The Reynolds stresses are assumed to be linearly related to the rate of strain as

$$\overline{\rho}\widetilde{u_i''u_j''} = \frac{2}{3}\delta_{ij}\underbrace{\left\{\overline{\rho}k + \mu_t\frac{\partial \tilde{U}_k}{\partial x_k}\right\}}_{3} - \mu_t\left\{\frac{\partial \tilde{U}_i}{\partial x_j} + \frac{\partial \tilde{U}_j}{\partial x_i}\right\}. \tag{21}$$

Three versions of the two-equation $k-\varepsilon$ model are investigated:

- model 1 is the incompressible $k-\varepsilon$ - model, in which no terms within the underbraces appears.
- model 2 is the commonly used $k-\varepsilon$ model in variable density flow, and it accounts for acceleration (term 1) and dilatation effects (term 3). The acceleration term appear in variable density flow, as fluid with low density is preferentially accelerated relative to fluids of high density by the mean pressure gradient. The dilatation term is owing to the heat release, which causes the fluid to expand and accelerate.
- model 3 is the ε-equation derived from the expression of conservation of angular momentum during compression, which, in addition to term 1 and term 3, yields a new term (term 2). The constant C_4 is consequently assigned a value so that the turbulent angular momentum is conserved.

The turbulent eddy viscosity is obtained on dimensional grounds from

$$\mu_t = C_\mu\overline{\rho}\frac{k^2}{\varepsilon}, \tag{22}$$

and for the turbulent scalar fluxes a gradient model is employed

$$\overline{\rho}\widetilde{u_j''\Phi_a''} = -\frac{\mu_t}{\sigma_t}\frac{\partial\tilde{\Phi}_\alpha}{\partial x_j}. \tag{23}$$

The turbulence contants have been assigned the following values:

$C_\mu = 0.09,\ C_1 = 1.44,\ C_2 = 1.92,\ C_3 = 1.25,$
$C_4 = -0.333,\ \sigma_k = 1.0,\ \sigma_\varepsilon = 1.3,\ \sigma_t = 0.7.$

3. COMPUTATIONAL DETAILS

3.1 The solution procedure

In this study a modified TEACH-T (ref. 7) code is used, where the SIMPLE algorithm is employed to solve the differential equations outlined in Section 2 (ref. 8). The equations are discretisized using a hybrid central/upwind finite difference formulation, where the upwind scheme is used when the local Reynolds mesh number is greater than two for the convection terms, and the central scheme otherwise. Staggered grids are used for the velocities, and the continuity equation is rewritten into an equation for pressure correction, which is used to correct the pressure and the velocities.

3.2 Experimental setup and boundary conditions

As a test case, a two dimensional model combustor geometry has been chosen, and the predictions are compared with experimental data (ref. 9). The lenght, L, of the combustor is 1.7m, and the diameter, D, is 0.1223m. The fuel (taken as pure methane in the calculations) enters the cylindrical combustion chamber in a central jet stream surrounded by a faster-moving coaxial air stream (Fig. 1). The inner radius of the fuel, R_{fuel}, and air, R_{air}, inlets are 0.0295m and 0.0465m, respectively. The mass flow rates are 7.2g/s in the fuel stream and 137.0 g/s in the air stream, which yields an air/fuel velocity ratio of approximately 20:1.

The configuration is axisymmetric and therefore the cylindrical form of the conservation equations is employed. A 60x60 non-uniform grid is used, with a higher node concentration in the axial direction near the inlet. In the radial direction special attention has been paid to the mixing region between the fuel and the air stream, where an annulus mixing layer is formed. To ensure that all radial gradients are resolved, the grid has been made highly dense in that particular area. The calculation domain has been extended upstreams into the air and fuel ducts, as the measurements indicate that the recirculation zone produced downstream of the fuel injector duct may penetrate up into it.

At the inlets uniform profiles are prescribed as, in the experimental setup, porous-metal discs were installed in the fuel injector and in the air entry sections to provide uniform inlet flows.

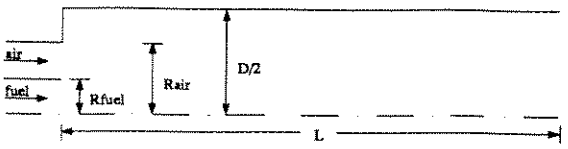

Fig. 1 Configuration.

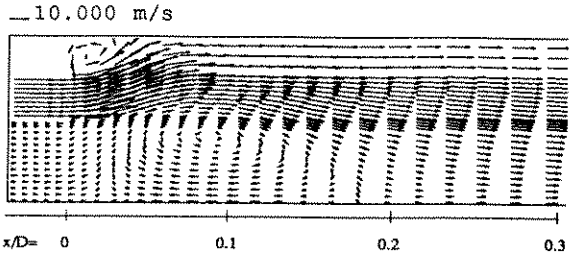

Fig. 2 Vector plot of the axial velocities in the initial mixing region.

As no information about the turbulence quantities were obtainable from the experimental data empirical expressions have to be given:

$$k_{in} = AU_{in}^2 \tag{24}$$

$$\varepsilon_{in} = C_\mu k_{in}^{1.5}/(0.03l). \tag{25}$$

The constant A has been assigned two different values at the air and fuel inlets to examine the effects of the inlet turbulence intensity on the combustion models, and the turbulence intensity, I (taken as $\sqrt{k}/U$ in the calculations), has been set to 7 % and 17 % in the calculations. The length scale l in equation (25) is taken as the radius of the fuel inlet, and as the annular height of the air inlet. The variance of the mixture fraction is set to zero at both inlets.

The combustor walls are water-cooled, and the temperature is taken from the experiments as T_w=500K. Standard wall functions are used to treat the near-wall regions.

At the axis of symmetry, zero gradients are imposed except for the radial velocity which is set to zero. The outlet condition is that axial gradients for the dependent variables should vanish.

4. RESULTS AND DISCUSSION

Steady calculations of a turbulent reacting flow have been carried out. Two fast-chemistry combustion models have been analyzed, and three different $k-\varepsilon$ turburbulence models are investigated. The

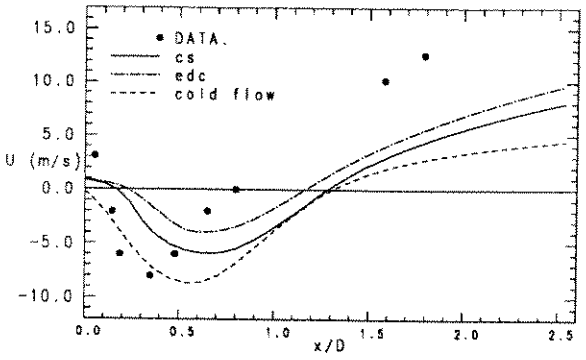

Fig. 3 Axial velocity distribution at symmetri axis.

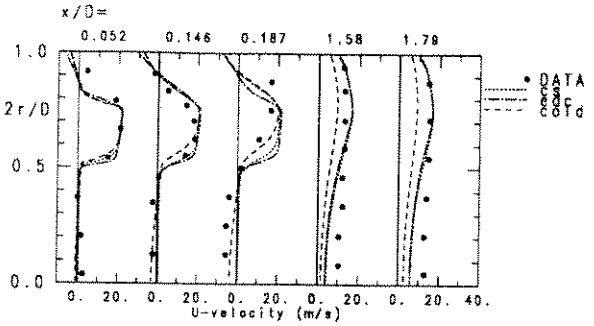

Fig. 4 Measured and calculated axial velocity profiles (I=17% and model 3).

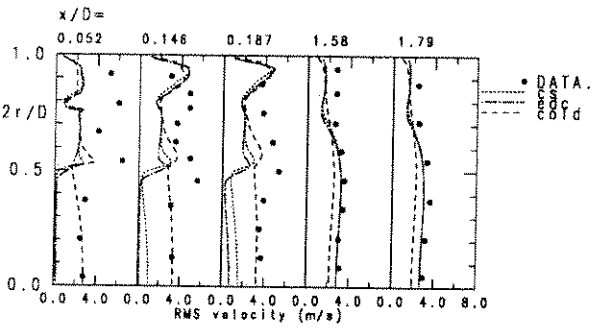

Fig. 5 Measured and calculated fluctuating axial velocity profiles (I=17% and model 3).

calculations have been compared with temperature, mean and turbulent flow fields measurements in a non-premixed, axisymmetric combustor without swirl.

Flame stabilization was achieved by a high momentum flux ratio of the air and fuel streams, which produces a recirculation zone immediately downstream the fuel inlet (Fig. 2). Another zone of negative velocities appears near the outer wall owing to the sudden expansion of the combustor.

Generally, independent of the chemistry model used, the length of the recirculation zone is overpredicted, and the negative velocities and the strength of the recirculation zone are underpredicted. Fig. 3 shows the axial velocity distribution at the symmetry line, and it is seen that when using the EDC chemistry model the maximum negative velocities that appear in the recirculation zone are underpredicted by more than a factor of two in the combusting calculations. The CS chemistry model is in better agreement with data: here the maximum value of the negative velocity is about 75 % of the measured value. The length of the recirculation zone is overpredicted by $\approx$ 30 % with the EDC model and by $\approx$ 50 % by the CS model. Some of these discrepancies between predictions and measurements could be related to numerical errors and to the turbulence model, but they are probably mainly due to the steady state assumption. High-speed pictures of the reacting flow field in the experiments show significant fluctuations in the turbulent structure, and that large scale motions, originating from the unsteady mean flow, are present. These unsteady large scale motions also have a significant influence on the velocity fluctuations and the mean temperature field. It should also be noticed that the mean velocity profiles were measured with the aid of laser Doppler anemometer, and the experimental errors estimated to 5 %, except in the vincinity of the recirculation zone where errors increase to 30% .

The effects of heat release on the mean velocity field are shown in Fig. 4. The heat release causes the flow to expand and accelerate. For comparison the cold flow calculations are also included. The volume occupied by the recirculation zone and the strength are decreased, as compared with isothermal flow. Even if the main reason for the errors probably originates from the steady state assumption, the turbulence model fails to predict the turbulence in this region, where the turbulence is strongly affected by streamline curvature effects.

A comparison of the axial rms values from cold and hot flow calculations with exprimental at five different axial locations, is shown in Fig. 5. The data indicate high axial rms values in the central recirculation zone, but although the peak values occur in the shear layers where the maximum velocity gradients are, the rms values do not scale with the velocity gradient. Therefore, it is seems that the most of the rms velocities in the central regions in the experiments primarily arise from the large scale motion. Generally, the calculated levels of fluctuations in the recirculation zone are much lower than measured quantities. The CS model again performs better, and the fluctuating velocities in the recirculation zone are $\approx$ 40 % of the measured quantities at x/D=0.052 and increase

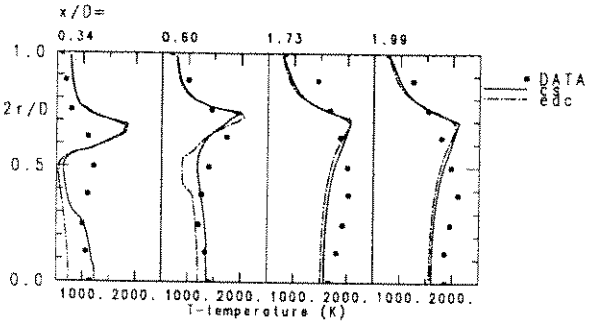

Fig. 6 Measured and calculated temperature profiles (I=17% and model 3).

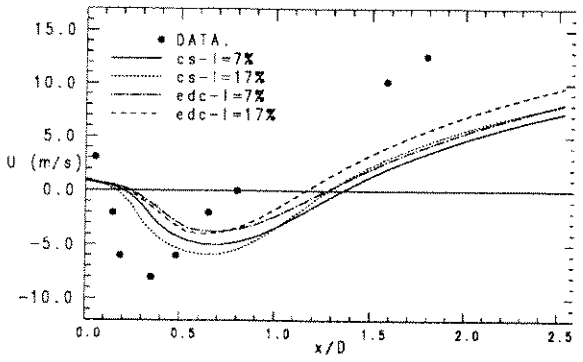

Fig. 7 Axial velocity distribution at symmetri axis for the chemistry models, when inlet turbulence intensity is varied (model 3).

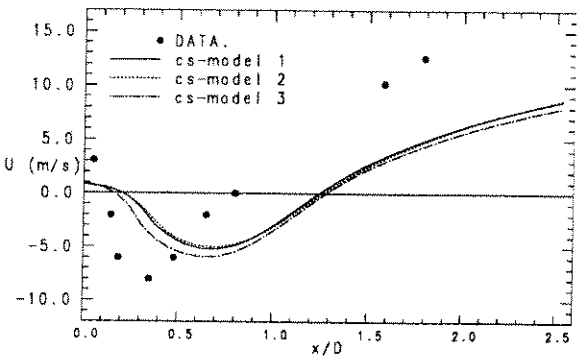

Fig. 8 Axial velocity distribution at symmetri axis for different turbulence models (I=17%).

to $\approx$ 50 % at x/D=0.187. The EDC model poorly predicts the fluctuating velocities and the corresponding values are $\approx$ 10 % at x/D=0.052 and $\approx$ 20% at x/D=0.187. Further downstream, where the effects of the motions in the recirculation zone diminish, the agreement is much better. The energy released has the effect of lowering the levels of fluctuating velocities, both in the recirculation zone and in the annular shear layer, where the peak values are reduced by $\approx$ 25% in the combusting calculations. One can also observe that the strength of the recirculation zone clearly scales with the levels of fluctuating velocities.

The radial temperature distribution for the two chemistry models is shown, at four different axial locations, in Fig. 6. The CS model predicts a higher temperature at the center line in the recirculation zone (x/D=0.34 and x/D=0.60) than the EDC model, and the values are closer to the measured ones. This is associated with the stronger wake in the CS model calculations, as more energy released in the chemical reaction is drawn to the centeline by the fluid in the recirculation zone. Further downstream (x/D=1.73 and x/D=1.99), the effects of the recirculation zone have decreased, and both models predict almost the same temperature profiles. Both models overpredict the temperature in the mixing layer, and a very steep temperature gradient prevails in the calculations compared with the data. Again, this is related to the large scale fluctuations. In the experiments, the mixing is mainly due large scale motion, and the temperature gradient is thus much smoother, as the reacted zones are rapidly mixed with non-reacted. This is not the case in the calculations, owing to the steady state assumption.

The sensitivity to inlet turbulence intensities has been examined, and in Fig. 7 the distributions of axial velocities are shown for both chemistry models. They show that an increase in turbulent intensity at the inlets will increase the strength of the wake, and that the length of wake decreases. These effects are more pronounced when the CS chemistry model is used, where velocities are reduced up to 20%, and the length of the recirculation zone is decreased about 5 %. The EDC model does not respond as much: the maximum negative velocity is almost unchanged, but the length of the recirculation zone is decreased by 10 % .

A comparison between the three turbulence models is shown in Fig. 8. It can be seen that the effects of the additional acceleration and dilatation terms included in model 2 are very small in the present case: the velocities are slightly increased in the recirculation zone, and the length of the recirculation zone is very little increased. However, with model 3 the predictions of the axial mean velocities was significantly changed in the recirculation zone. This results in an improvement of the calculated axial velocities in the recirculation zone as compared with experiments, with up to 20 % increased axial backflow velocities. The

length of the recirculation zone is increased by $\approx 8\%$.

5. CONCLUSIONS

Generally in the combusting calculations, in the present study, the strengths of the mean and fluctuating velocity flow fields are underpredicted in the initial mixing region. Agreement is much better further downstream. These discrepancies are attributable to the steady state assumption, as the mean flow in the experiments has been found to be unsteady, and as large scale structures are present in the initial mixing region.

Significant differences in the predictions were obtained in the initial region, where large velocity fluctuations prevail, depending on whether the CS model or the EDC model was used. The overall performance of the CS model was much better than that of the EDC model. It could therfore be concluded, when calculating highly turbulent reacting flows, that it is necessary to account for the effect of turbulence on concentration fluctuations. This is especially important when the mean density is determined, as it couples the thermochemical aspects of the flow to the fluid-mechanical ones.

Sensitivity to changes in the inlet turbulence intensity was examined. It was found that an increase in inlet turbulence intensity yielded a stronger wake, and that its volume decreased. These effects were much more pronounced for the CS model. This, again, indicates the need of including the effects of concentration fluctuations in the calculations.

Three types of $k - \varepsilon$ models have been examined. When the incompressible turbulence model (model 1) was extended to include effects of acceleration and dilatation (model 2) owing to variable density, the predicted flow field was altered very little. A new ε-equation, derived from the expression for conservation of turbulent angular momentum (model 3), resulted in an improvement of the calculated recirculation zone as compared with experiments, with increased axial backflow velocities with up to 20% .

REFERENCES

1. J. Chomiak, Rept. 88/12, Dept. of Thermo and Fluid Dynamics, Gothenburg, 1988.
2. B.F. Magnussen, in: D.C. Siegla and G.W. Smith (Ed.), General Motors Symposium on Particulate Parbon Formation During Combustion, Warren, USA, October 14-16, 1980, Plenum Publishing Corporation, 1981, pp. 321-341.
3. R.W. Bilger, in: P.A. Libby and F.A. Williams (Ed.), Turbulent Reacting Flows, Springer Verlag, Berlin, 1980, pp. 65-113.
4. W.P. Jones and J.H. Whitelaw, Combustion and Flame, 48 (1982) 1-82.
5. N. Mechitoua and P.L. Viollet, in: G. Hetsroni (Ed.), 9th International Heat Transfer Conference, Jerusalem, Israel, August 19-24, 1990, Hemisphere Publishing Corporation, New York, 1990, Vol. 4, pp. 375-380.
6. J. Nisbet, Rept. 91/12, Dept. of Thermo and Fluid Dynamics, Gothenburg, 1991.
7. L. Davidson and P. Hedberg, Rept. 86/13, Dept. of Thermo and Fluid Dynamics, Gothenburg, 1986.
8. S.V. Patankar, Numerical Heat Transfer and Fluid Flow, McGraw-Hill, Washington, 1980.
9. F.K. Owen, L.J. Spaddacini and C.T. Bowman, Rept. EPA-600/2-76-247a, Washington, 1976.